Checking simulations of a geolithological model obtained by means of nested truncated bigaussian method

Claudia Cherubini, Fausta Musci, Nicola Pastore

Abstract- Characterizing the spatial distribution of major lithotypes and their relationships is a key aspect in the process of hydrogeological modeling of aquifers in that assignment of lithotypes-specific hydraulic and hydrochemical properties requires the knowledge of the layout of the lithotypes themselves.
Truncated bigaussian simulation is a procedure derived from the truncated Gaussian model, used to simulate random sets, and, in particular, variable geological characteristics, expressed as categorical variables. Anyway, in cases of many lithotypes having not homogeneous spatial behaviors, this methodology might not explain at best the relations existing among the lithotypes themselves; a more general method is therefore required to represent this variability.
In this paper, that concerns a site whose geologic asset has already been reconstructed, in order to better characterize the aquifer geolithological architecture, nested simulation for a macro-unit of the previously realized geolithologic model has been carried out, together with a check phase of the results obtained by the mentioned simulation.
The proposed methodology can represent a useful instrument for the modeling of complex geological layouts other than in the detailed characterizations of hydrogeological studies, for a better interpretation of the complex phenomena that take place in groundwater circulation and contaminant propagation.

Keywords**—**nested truncated bigaussian simulation, lithotypes, geolithologic characterization, check

I. Introduction

Hydrogeological modeling requires an accurate characterization of the aquifer in terms of its lithological architecture, that is to say the spatial layout of these different lithotypes within the reservoir.

Truncated bigaussian simulation is an extension of truncated Gaussian method that retains the main advantages of the latter but overcomes its limitations; it is more flexible than the truncated Gaussian simulation and allows more complex transitions between lithotypes. It represents a new and effective procedure of reproducing complex geometrical attributes of a reservoir by means of simulating several lithotypes with different spatial structures and taking into account their global proportions.

The method is based on the relationship between indicator variables from lithotypes distribution and the Gaussian random functions chosen to represent them, with the compromise of having equivalent geostatistical behavior. Geological information is incorporated to the model by the definition of the indicator variables, their truncation strategy and the lithotypes proportions.

A critical limitation arising in this methodology is that, in cases of a consistent number of lithotypes it only produces simulations where the examined lithotypes are sequentially ranked. In other words, when there is the presence of 4 or more of them, and all are in contact with one another, the definition of the lithotype rule might not explain at best the relations existing among all of them [1].

In cases of complicated contacts among lithotypes, due to the great variability of their distribution within the aquifer, it is necessary to allow contacts between all of them by means of the use of more than two gaussian random functions or to find a more general method to represent this variability.

In the study case the aim is that of characterizing in detail the lithotypes present that show different hydraulic and environmental behavior. The applied method is the hierarchization of the degree of anisotropy of some intrinsic characteristics of the same sedimentary formation such as degree of cementation, of diagenesis and of fissuration.

Starting from the results of a previous study [2], in this paper a nested truncated bigaussian method is applied and checked in order to set up a geolithological reconstruction of an aquifer.

II. Materials and Methods

A. Case study: Specific geologic features

The study area, whose name cannot be explicitly mentioned for privacy reasons, belongs to a wide industrial district whose geological and hydrogeological characterization has already been examined in previous studies [2], [3] and [4].

The area corresponds to a huge tectonic depression of the Mesozoic carbonatic rocks that opens towards the Adriatic Sea. This depression has been filled up by the deposits of the sedimentary cycle of the Bradanic Trough constituted by sandy-calcarenitic deposits (Pliocene-lower Pleistocene) locally recognized as “Calcareniti del Salento”. In almost all

Manuscript received April 25, 2009: Revised version received May, 2009.
Claudia Cherubini is with Dipartimento di Ingegneria Civile e Ambientale Politecnico di Bari Via Orabona 4, 70100 Bari, ITALY (phone: 0039356881198, fax: 00390805481878, e-mail claudia.cherubini@poliba.it).
Fausta Musci is with Dipartimento di Ingegneria Civile e Ambientale Politecnico di Bari Via Orabona 4, 70100 Bari, ITALY (e-mail: f.musci@poliba.it).
Nicola Pastore is with Dipartimento di Ingegneria Civile e Ambientale Politecnico di Bari Via Orabona 4, 70100 Bari, ITALY (e-mail: nicola.pastore.ing@gmail.com).

the investigated area are present, in continuity of sedimentation, not stratified banks of blue-gray clays characterized by intercalations of marls and/or calcareous sands. On the clayey formation there is the presence of Terraced Marine deposits constituted by clayey-sandy-calcarenitic both emerged and submerged shore sediment deposits, characterized by moderate thicknesses and sub-horizontal structural attitude. On them are detectable the olocenic continental deposits, of slender thicknesses, constituted by silts, marshy clays, river and dune sands. In the present study, the geolithologic modeling has concerned just the pleistocenic terraced marine deposits that constitute an aquifer in which groundwater flows in phreatic conditions, sustained by pliopleistocenic clays. For more in depth geological details reference can be made to Cherubini et al [2].

The specific geologic characteristics of the area have been evaluated from the stratigraphies of about 220 boreholes carried out on an area of about 6.5 km2. The boreholes have reached a maximum depth of 25 m from the sea level, for an average thickness of about 40 m, involving exclusively the shallow aquifer.

The soils belonging to the study area, on the basis of their lithostratigraphic characteristics have been grouped into the following five principal lithologic unities reported from the top to the bottom (Fig 1), after a shallow layer of anthropic material.

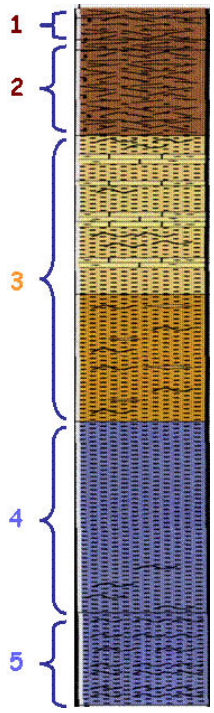

Fig. 1: Stratigraphic column characteristic of the area with principal lithologic unities

Filling material has a medium thickness variable generally from 0 and 2.5 m, with maximum thicknesses equal to 6 m from the ground level. It is constituted by elements of various grain sizes and locally fragments of concrete and bricks are detectable.

Alluvial and colluvial deposits (Holocene) have an average thickness variable generally from 0.5 to 5 m from the ground level. They are constituted by layers of sand, silt, silty sands and sandy silt, clayey silts and silty clays; especially on the basal part they are rich in carbonatic concretions.

Terraced marine deposits (Middle-Upper Pleistocene) are characterized by intercalations of fractured and weathered calcarenitic levels and fine sand and at times silty sand or sandy silt locally are present intercalations of lenses of clayey silts. These deposits host the shallow aquifer and have an average thickness of the order of 12-18 m from the ground level.

Silty sands of the middle Pleistocene are constituted by sands, sandy silts and silty sands of gray color. The silty fraction increases with depth together with the decrease of the sandy fraction. This deposit constitutes the top of the aquiclude.

Subapennine blue-gray clays (Lower Pleistocene) are characterized essentially by gray clays that are detectable at depths higher than 26 m and constitute the aquiclude that sustains the shallow aquifer.

B. Methodology of analysis

The Truncated Plurigaussian simulation consists in defining several underlying Gaussian Random Functions (GRF), which are truncated at different thresholds, on the basis of the proportions of each lithotypes [5].

Although the method could use an unlimited number of Gaussian functions, in practice it is reduced to 2 (denoted Y1 and Y2) for the simplicity of analysis in the Gaussian field. These two functions can be independent or correlated:

$$\begin{aligned} Y_1 &= W_1 \\ Y_2 &= \rho W_1 + \sqrt{1-\rho^2} W_2 \end{aligned} \tag{1}$$

where W1 and W2 are two independent GRF and ρ is the correlation coefficient between Y1 and Y2 [6].

Each lithotype, denoted by different random sets Bi, is obtained by truncating the two GRF at given thresholds (denoted ti,j and si,j respectively for the lower and upper bounds of the GRF "j" for the lithotype "i"):

$$x \in B_i \Leftrightarrow \begin{cases} t_{i,1} \le Y_1(x) \le s_{i,1} \\ t_{i,2} \le Y_2(x) \le s_{i,2} \end{cases} \tag{2}$$

with i = 1,…, N and N = number of lithotypes to be simulated. The thresholds are determined experimentally in function of the proportions pi of each lithotype in space. This, in practice, means considering the probability that a certain point lies in a given lithotype:

$$p_i(x) = E\{I_i(x)\} = \Pr\{t_{i,1} \le Y_1(x) \le s_{i,1} \cap t_{i,2} \le Y_2(x) \le s_{i,2}\} = \\ = \int_{t_{i,1}}^{s_{i,1}} \int_{t_{i,2}}^{s_{i,2}} g_\Sigma(u,v)\, du\, dv \tag{3}$$

where $g_\Sigma(u,v)$ is the standard bivariate Gaussian density function, coming from:

$$f(x_1,...,x_N) = \frac{1}{(2\pi)^{\frac{N}{2}} |\Sigma|^{\frac{1}{2}}} \exp\left(-\frac{1}{2} (\bar{x} - \bar{1}\mu)^T \Sigma^{-1} (\bar{x} - \bar{1}\mu) \right) \tag{4}$$

with the vector of mean equal to 0 ($\bar{1}\cdot\mu=\bar{0}$) and $\Sigma=\begin{pmatrix}1 & \rho\\ \rho & 1\end{pmatrix}$= correlation matrix for the bivariate case.

When the two GRF are independent, the eq.3 can be factorized:

$$p_i(x)=\left(\int_{t_1^i}^{s_1^i} g(u)\,du\right)\times\left(\int_{t_2^i}^{s_2^i} g(v)\,dv\right)= \\ =\left(G(s_1^i)-G(t_1^i)\right)\times\left(G(s_2^i)-G(t_2^i)\right) \tag{5}$$

where, simply, $g(u)$ and $g(v)$ are the standard normal density function and so G(s) and G(t) are the cumulative normal distribution functions.

The partition of bigaussian space presented in plan view is usually referred to as the lithotype rule: Y_1 is plotted on the horizontal axis and Y_2 on the vertical axis, each rectangle representing a lithotype (Fig.2). It is possible to assign the lithotypes in different ways, in order to better control lithotype transitions and settings.

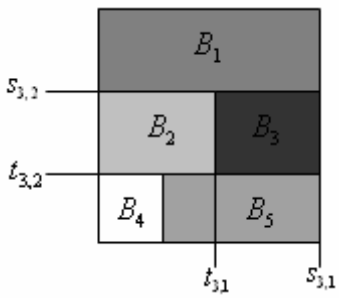

Fig. 2: Lithotype rule

The truncation rule controls the transitions between the different lithotypes. It has to be chosen in accordance with the geological evidence and interpretation of the deposit and with the statistical behavior of the data. Here, two independent standard Gaussian random fields (denoted by Y_1 and Y_2) will be used, so the truncation rule amounts to defining a partition of the bi-Gaussian space [7].

Truncating these variables creates indicators, so as to mimic the spatial behavior of the different lithotypes:

$$I_i(x)=\begin{cases}1 & \text{if } x\in B_i\\ 0 & \text{otherwise}\end{cases} \tag{6}$$

In order to define the structures of the two GRF, and to carry out the simulations, their relation with indicators has to be considered, which uniquely links their covariances. In fact, from the experimental data, simple and cross-variograms are obtained for all the indicators that represent the different lithotypes:

$$\gamma_{B_i}(x,x+h)=\frac{1}{2}E\left[I_{B_i}(x)-I_{B_i}(x+h)\right]^2 \tag{7}$$

$$\gamma_{B_iB_j}(x,x+h)=\frac{1}{2}E\left\{\left[I_{B_i}(x)-I_{B_i}(x+h)\right]\times\left[I_{B_j}(x)-I_{B_j}(x+h)\right]\right\} \tag{8}$$

Considering, for the moment, just the simple variogram (7) and introducing the covariance C_1 and C_2 of the gaussian functions at distance h, it could be written:

$$\gamma_{B_i}(x,x+h)=\frac{1}{2}\left\{E\left[I_{B_i}(x)\right]+E\left[I_{B_i}(x+h)\right]-2E\left[I_{B_i}(x)\times I_{B_i}(x+h)\right]\right\}$$

and from (3) and (4):

$$\gamma_{B_i}(x,x+h)=\frac{1}{2}\Big(p_i(x)+p_i(x+h)- \\ -2\int_{t_{i,1}(x)}^{s_{i,1}(x)}\int_{t_{1,2}(x)}^{s_{1,2}(x)}\int_{t_{i,1}(x+h)}^{s_{i,1}(x+h)}\int_{t_{i,2}(x+h)}^{s_{i,2}(x+h)} g_\Sigma(u_1,u_2,v_1,v_2)\,du_1du_2dv_1dv_2\Big) \tag{9}$$

with $\Sigma=\begin{pmatrix}1 & \rho & C_1 & \rho C_1\\ \rho & 1 & \rho C_1 & C_2\\ C_1 & \rho C_1 & 1 & \rho\\ \rho C_1 & C_2 & \rho & 1\end{pmatrix}$ = covariance matrix

for 4 variables case.

In the same way, for the cross-variograms it could be written:

$$\gamma_{B_iB_j}(x,x+h)= \\ -\frac{1}{2}\int_{t_{i,1}(x)}^{s_{i,1}(x)}\int_{t_{i,2}(x)}^{s_{i,2}(x)}\int_{t_{j,1}(x+h)}^{s_{j,1}(x+h)}\int_{t_{j,2}(x+h)}^{s_{j,2}(x+h)} g_\Sigma(u_1,u_2,v_1,v_2)\,du_1du_2dv_1dv_2+ \\ +\int_{t_{i,1}(x+h)}^{s_{i,1}(x+h)}\int_{t_{i,2}(x+h)}^{s_{i,2}(x+h)}\int_{t_{j,1}(x)}^{s_{j,1}(x)}\int_{t_{j,2}(x)}^{s_{j,2}(x)} g_\Sigma(u_1,u_2,v_1,v_2)\,du_1du_2dv_1dv_2 \tag{10}$$

Thus, the procedure of variographic analysis starts from calculating the experimental indicator direct and cross-variograms from the lithotypes data, then the two gaussian variables come into play. Using an iterative approach, the parameters of the covariance model of the two underlying GRF are tested, in order to generate an indicator variogram model which fits in the best way the experimental indicator variograms [8]. Once the variogram model has been determined, it is possible to perform the conditional simulations that proceed with the following three steps [7]:

★ Conversion of the conditioning information (experimental lithotypes data) into multigaussian values at data points, in respect of the gaussian covariance models, the multigaussian spatial distribution and the thresholds imposed by lithotype rule. This step is performed by an iterative technique known as the Gibbs sampler [9]. This algorithm starts by assigning randomly gaussian values to the data points, according with the thresholds that characterize each lithotypes in the lithotype rule, but not with their covariance. Thus, to obtain the correspondence also with the gaussian covariance models, in turn, each experimental point is discarded and estimates by kriging the gaussian values of the other data and combining the values with the residuals obtained at each iteration. The new values of Y_1 and Y_2 in the experimental point α can be defined from:

$$Y_1(\alpha) = Y_1^*(\alpha) + \sigma_1^*(\alpha) \times R_1(\alpha)$$
$$Y_2(\alpha) = Y_2^*(\alpha) + \sigma_2^*(\alpha) \times R_2(\alpha)$$

where $Y_1^*(\alpha)$ and $Y_2^*(\alpha)$ are the simple kriging estimates, $\sigma_1^*(\alpha)$ and $\sigma_2^*(\alpha)$ the standard deviation of those estimations, $R_1(\alpha)$ and $R_2(\alpha)$ the residuals according to the standard normal variable and lying in the intervals defined by the threshold values.

★ Conditional simulations of Y_1 and Y_2, using the gaussian values assigned in the previous step as conditioning data, at the locations where the lithotypes realizations are required. The realizations can be obtained using any Gaussian simulation algorithm, such as the turning band algorithm or the sequential Gaussian simulation algorithm [10].

★ Truncation of the two gaussian variables at each point of the simulated multigaussian field, according to Eq. 2, in order to produce lithotype information.

III. Problem Solution

A. Bi-gaussian simulation

The first step of this study is that of constructing a 3D model that would discretize the subsoil into the previously described 5 lithological units. These layers have been, then, further characterized in function of the hydraulic behavior of the lithotypes present.

LITHOLOGIC UNIT	LITHOTYPE
I. Alluvial and colluvial deposits (Olocene)	1. Silt
	2. Sandy silt and silty sand
	3. Sand
	4. Clayey silt and silty clay
II. Terraced marine deposits (Middle-Upper Pleistocene)	5. Calcarenitic levels
	6. Sand
	7. Sand with inclusions of calcarenite
	8. Sandy silt and silty sand
	9. Silt, clayey silt, silty clay and clay
III. Silty sands of the middle Pleistocene	10. Sand
	11. Silty sand and sandy silt
	12. Silt
IV. Subapennine blue-gray clays (Lower Pleistocene)	13. Clay

Table 1: Lithological unities and corresponding lithotypes.

In Table 1 the lithologic unities and the corresponding lithotypes taken into account are indicated. Neglecting the last lithologic unity, because only constituted by one lithotype, the other three unities have been separately characterized.

In practical terms, the procedure consists in creating three different working grids, in which are stored the boreholes and the units split by the boundary surfaces created by the initial interpolation. These grids are flattened, that is to say the information is transformed back to the sedimentation stage, as to improve the horizontal correlation. After the simulations, the different working grids are merged and back transformed into the original grid.

For each lithologic unit, the proportions of the lithotypes are computed at each cell of the working grids, because they are one of the fundamental information used by plurigaussian modeling. They are expressed in terms of vertical proportion curves (VPC), representing the variation of the proportions along the vertical axis. To calculate these proportions more accurately, global proportions, and thus the stationariety of the proportions over the whole area, have not been considered. In fact, for each lithologic unit, according with the input borehole data, more VPC have been used, as to respect the local spatial distribution of the lithotypes more than the global one. The individuated VPC have been, thus, used as constraining information to calculate the proportions on the whole 3D grid through co-kriging estimation. In fact, for each macro-unit, the spatial behaviour in terms of proportions of every lithotype has been modeled with a single 2D model. Stationary models with very high range have been used, in order to consider them non-stationary in the area studied. Figure 3, 4 and 5 show the results of the computation of 3D proportions, for the different macro-units.

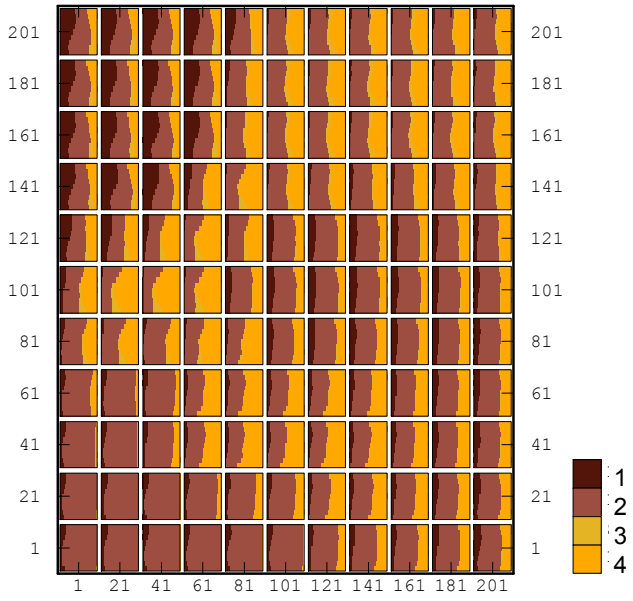

Fig. 3: 3D Proportions of the top unity.

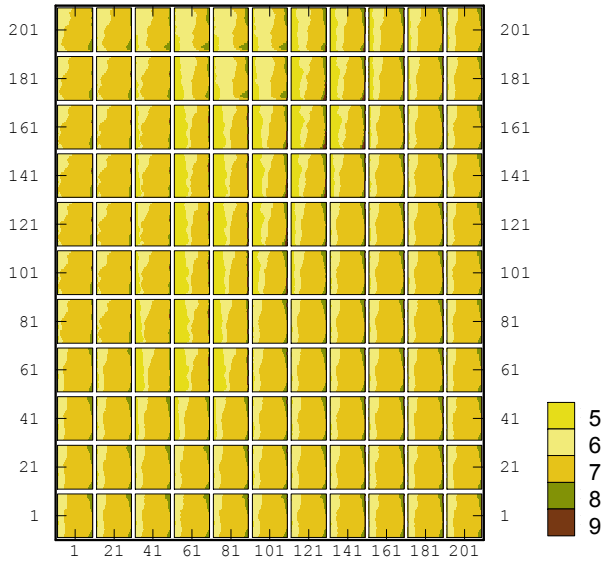

Fig. 4: 3D Proportions of the middle unity.

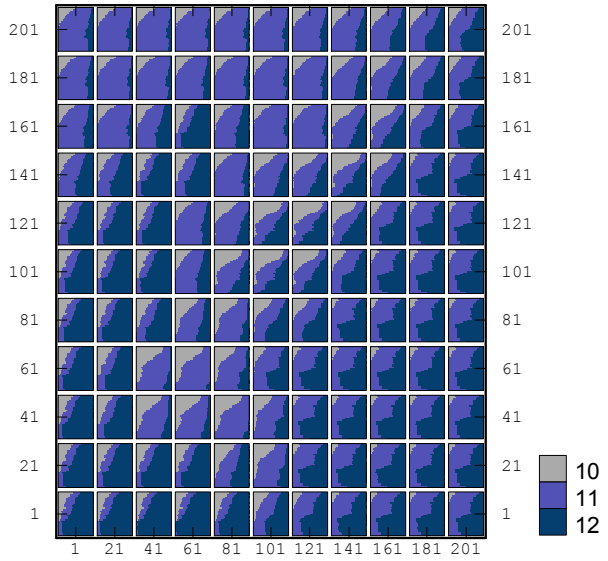

Fig. 5: 3D Proportions of the bottom unity.

Using the information coming from the previous maps (each little rectangle representing the mean VPC on 20 cells of the working grids), the simulation will keep in count the localization of the lithotypes. Thus, for the top macro-unit, lithotype nr.4 is absent in the south-western area, and nr.1 prevalent in the north-western area. In the middle macro-unit, the lithotype nr.5 and nr.9 are present just in the middle of the area. In the bottom macro-unit, in the eastern part of the area is very few the presence of lithotype nr.10, and in the north-west of nr.12.

The next step has been the plurigaussian variographic analysis, fundamental to define the lithotype rules and the models of the two GRF.

Figure 6 shows the lithotype rules for each lithologic unit, defined from the transition probabilities of the lithotypes, measured on the input data set, and geological information about the unit.

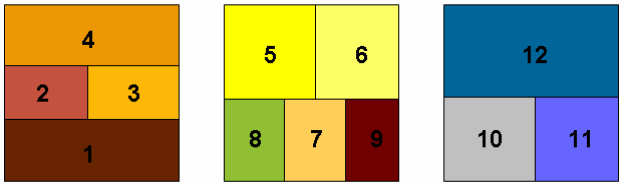

Fig.6: Lithotype rules for the three lithologic units.

In the first lithotype rule, corresponding to the first lithologic unit, no contact between lithotypes nr.1 (Silt) and nr.4 (Clayey silt and silty clay) has been imposed, according with transition probabilities. For the second unit (central lithotypes rule in fig.6), a forcing assumption has been made, due to the variable presence of the lithotypes within the unit. In fact, from the transition probabilities matrix, it appears that all the lithotypes are in contact with one another, and thus the variation is erratic. While, to define the transition rule, it has been assumed that lithotype nr.8 (Sandy silt and silty sand) is not in contact with nr.6 (Sand) and nr.9 (Silt, clayey silt, silty clay and clay) and lithotype nr.9 also with nr.5 (Calcarenitic levels). This choice depends on the fact that the transition probabilities between those lithotypes are however very low (smaller than 5%). Finally, for the third lithologic unit, the relative lithotype rule (the first on the right in fig.6) shows that all the lithotypes are in contact with one another.

Defined the rules of truncations and, thus, as GRF rule the spatial distribution of each lithotype, the next step consists in the trial and error phase in order to determine the structure of the variogram models of the two GRF that best fits the experimental indicator variograms. The table 2 shows the parameters used to define the models to use in the simulation phase, for each macro unity.

Figure 7 shows one conditional realization of the geolithologic domain obtained through plurigaussian simulation, using turning bands algorithm, and based on all the previous information.

In order to take into account the importance of the study in geological terms and for geological application, a filter has been applied on the initial simulation, to clean the noise from the image.

LITHOLOGIC UNITIES	MODELS	
	Y_1 structures	Y_2 structures
I. Alluvial and colluvial deposits	- Nugget - Cubic with ranges: X=250m, Y=200m, Z=4m	- Nugget - Cubic with ranges: X=250m, Y=180m, Z=4m
II. Terraced marine deposits	- Nugget - Spherical with ranges: X=150m,Y=300m,Z=6m	- Nugget - Cubic with ranges: X=130m, Y=300m, Z=4m
III. Silty sands of the middle Pleistocene	- Nugget - Cubic with ranges: X=150m, Y=100m, Z=8m	- Cubic with ranges: X=250m, Y=350m, Z=10m

Table 2: Parameters of the variogram models of each lithologic unit assigned to the two GRF Y_1 and Y_2.

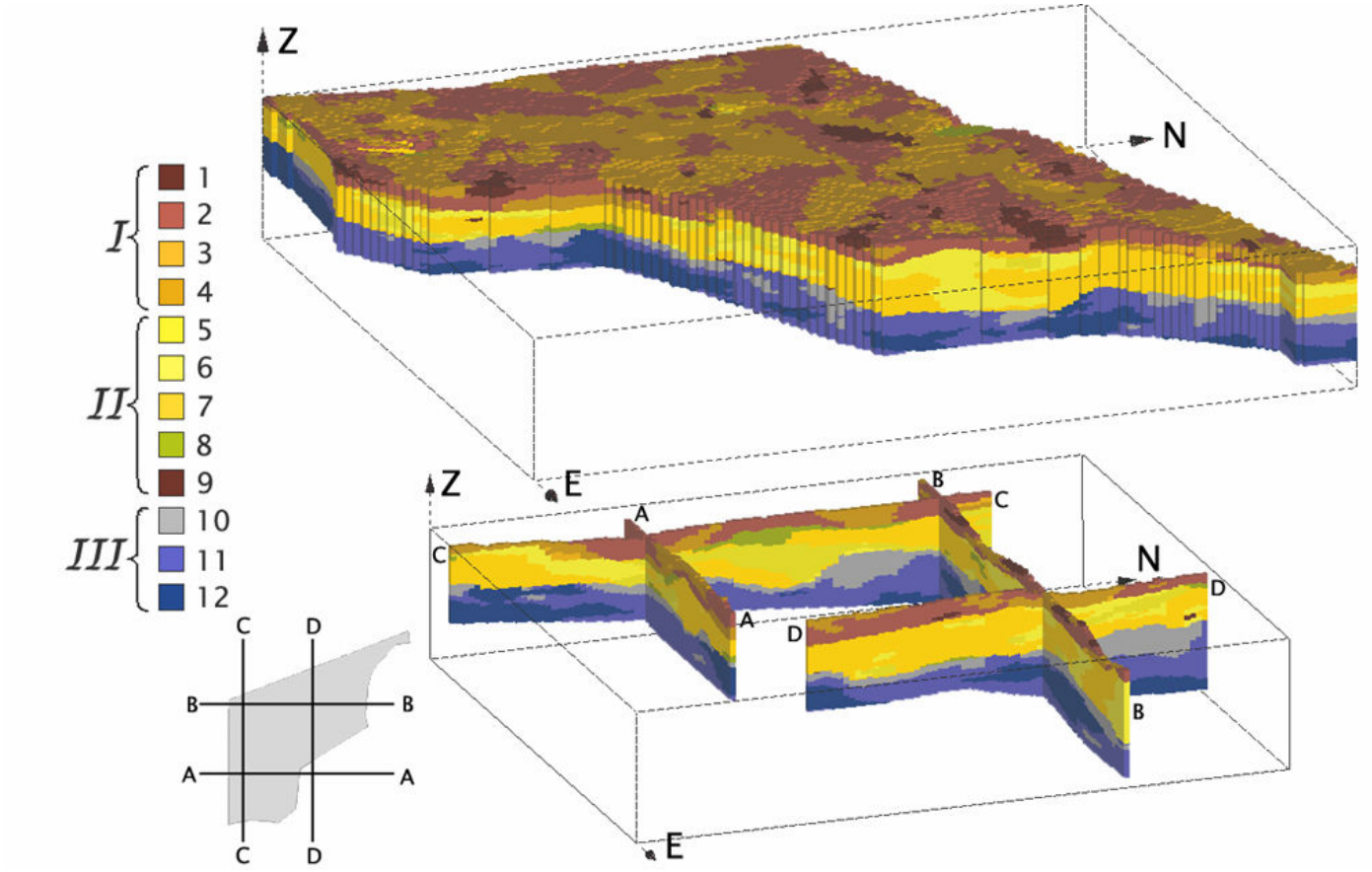

Fig. 7: Geological reconstruction.

B. Nested simulation

When there is the presence of 4 or more lithotypes, the definition of the lithotype rule might not explain at best the relations existing among the lithotypes. This is the case of the middle macro-unit: five lithotypes showing a variable distribution. Intuitively and as showed in [1], we can assume that it is impossible to represent the mutual contacts through the lithotype rule, in presence of five lithotypes all in contacts with one other.

The hierarchization of the degree of anisotropy of some intrinsic characteristics of the same sedimentary formation represents a way to overcome this limitation. In the present study, a nested simulation of one macro-unit has been carried out; this procedure has been realized in successive steps:

1. Plurigaussian simulation of the unit, considering just three lithotypes and, thus, amalgamating Calcarenitic levels (nr.5), Sand (nr.6), Sand with inclusions of calcarenite (nr.7) in a single new lithotype. The other two lithotypes remain Sandy silt and silty sand (nr.8) and Silt, clayey silt, silty clay and clay (nr.9). This choice depends on the big similarity of these lithotypes, in according with their formation processes, and on the difficulty of their precise identification from the stratigraphies.

2. Selection of the area where the simulation identifies the "amalgamated" lithotype.

3. Plurigaussian simulation of the three lithotypes, previously amalgamated, and back transformation in the selected area.

4. Union of the two previous simulations, to obtain together the initial five lithotypes.

In this way it is possible to consider the relationships between the lithotypes, even though it is not possible to condition these probabilities. This aspect has been considered negligible for the case study, due to the scarce proportion assumed by the lithotypes nr.8 and 9.

Moreover, in this way the model respects the anisotropies of some intrinsic characteristics of the different materials: soils with the same granulometry and different degree of anisotropy (degree of cementation, of diagenesis and of fissuration) have been grouped.

Thus, the inputs for the simulations have been:

- *Proportions of the lithotypes.*

For the first simulation, the scarce proportion of two of the three lithotypes evaluated, as mentioned before, has lead to consider the proportion stationary in the area, thus represented by the global VPC. It is shown normalized in figure 8, where it is possible to see the clear prevalence of the "amalgamated" lithotype, constituted by the sum of nr.5, 6 and 7, in terms of proportions compared to the nr.8 and 9.

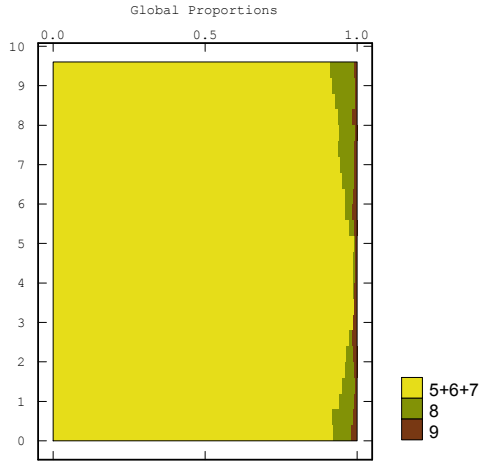

Fig.8: Global proportions of the middle unity discretized in three lithotypes.

For the successive simulation, the present heterogeneities have been taken into account by considering the non stationariety and computing the 3D proportions by co-kriging estimation. Again, stationary model with very high range has allows to obtain the result in figure 9.

Obviously, as in the previous simulation of the five lithotypes together, the lithotype constituted by Calcarenitic levels (nr.5) will appear just in the middle of the area: they come from the same stratigraphic columns.

- *Lithotypes rules.*

The lithotypes rule considered for the two simulations are taken in such a way that all the transitions are possible: between the "amalgamated" lithotypes and the other two, and between the three lithotypes previously amalgamated.

- *Variographic analysis.*

The variograms fitting, conducted separately for the two successive simulations, has resulted in defining the models of the two GRF used for simulating the spatial behavior of the nested lithotypes. In the first simulation, a nested variogram, composed by a nugget effect and a cubic model with ranges 250m, 300m and 6m, respectively for the N-S, W-E and vertical direction, has been fitted for the first GRF. The second model is composed by a nugget effect and a Gaussian model with ranges 200m, 250m and 7m in N-S, W-E and vertical directions. For the second simulation, the models used are spherical with ranges of 200m, 150m and 10m for the first GRF, and 200m, 300m and 12m for the second one.

On the basis of these input data, the two successive simulations have been carried on and then merged together.

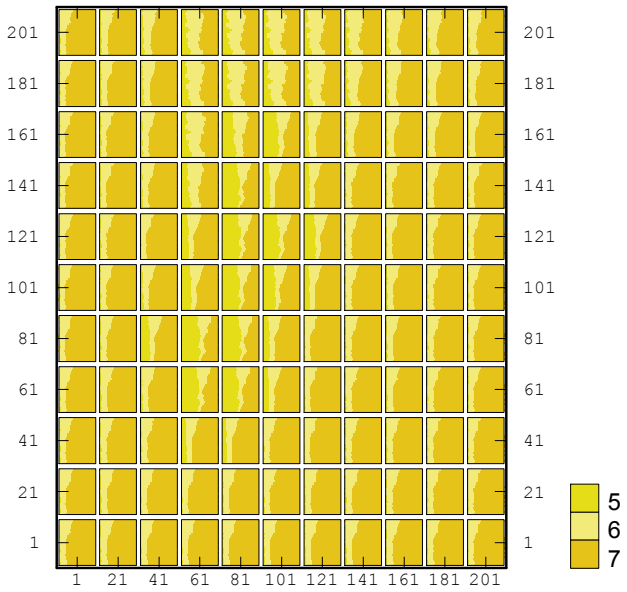

Fig. 9: 3D Proportions of the "amalgamated" unity.

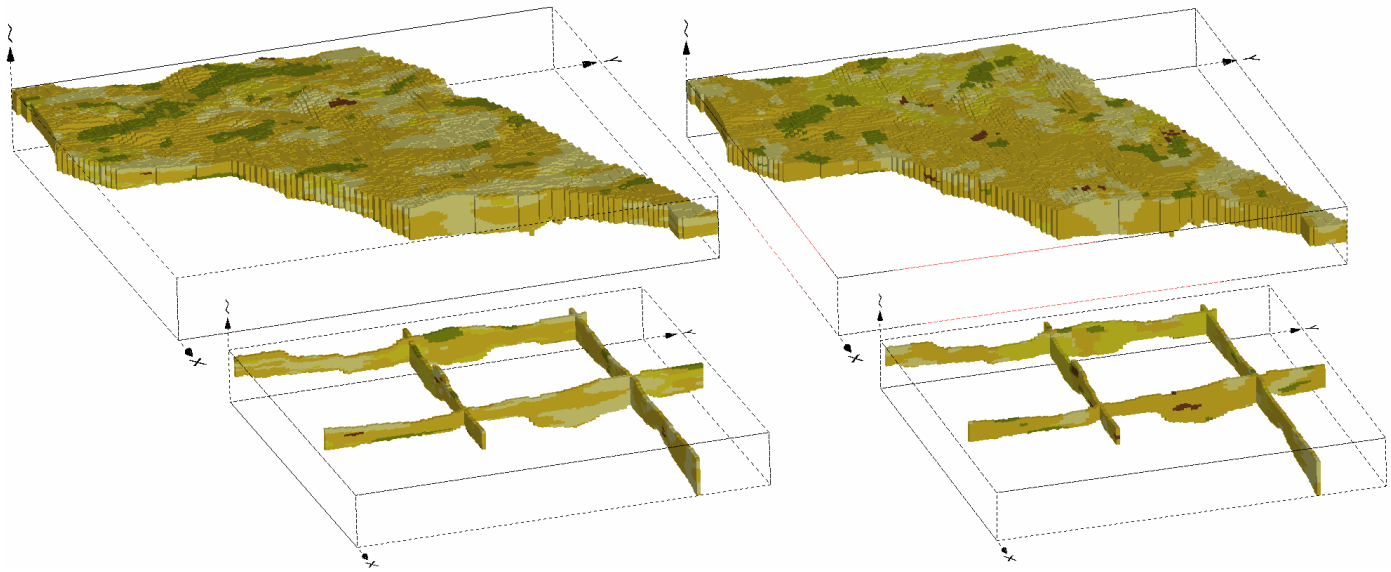

Fig. 10: Middle unit realizations obtained by nested and complete simulations.

Figure 10 shows one realization obtained by nested simulations and one by the initial one. The nested simulation procedure results in our study more correct, for various reasons. First, from a conceptual point of view, it permits to consider all the relationships between the lithotypes present. And in doing this, it doesn't proceed random, but allows through further discretizations of the strata to respect sedimentological and aspects of anisotropies of the lithotypes.

Moreover, observing figure 10, it is possible to see that the simulation made for successive steps aims at concentrating and representing the two lithotypes with scarce proportions (nr.8 and 9) as material lenses.

C. *Check the simulation*

On a single simulation it is possible to perform simple checks, comparing the histograms and the variograms of the simulated values with those one of the experimental data [11].

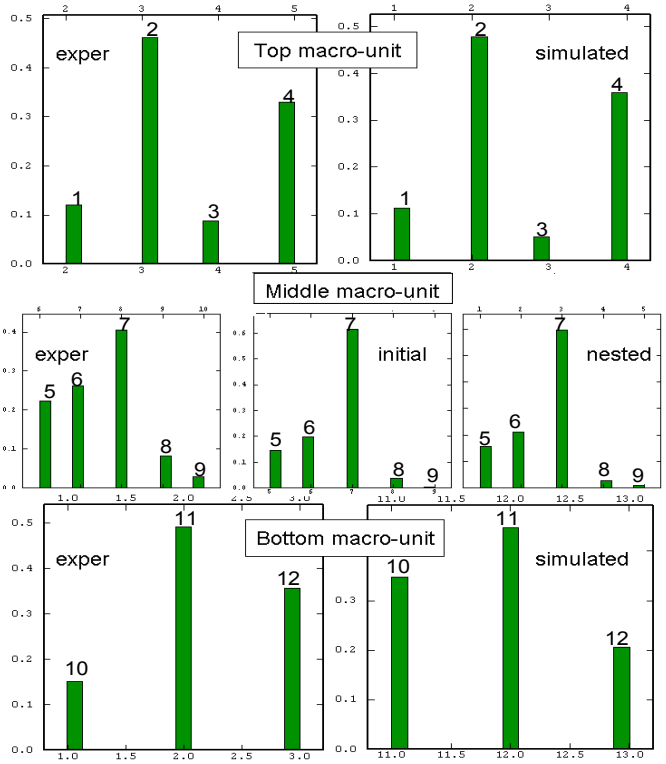

Fig. 11: Histograms of the experimental and simulated values, for each macro-unit.

As shown in the previous figure, the simulations, in general, well respect the initial distributions of the data, especially for the first macro-unit. For the second one, the simulations tend to increase the proportions of the lithotype constituted by Sand with inclusions of calcarenite (nr.7), although the relationships among the others remain the same. For the bottom macro-unit, the proportions of the lithotype constituted by Silty sand and sandy silt (nr.11) are well reproduced, while the other two are overestimated in one case, and underestimated in the other.

In order to check the initial and post-simulations variograms, indicator variables have been built for all the lithotypes. Thus, variograms have been calculated in two principal directions (N0 = North-South and N90 = West-east) on:

- ★ 351 original and 224,562 simulated values for the top macro-unit;
- ★ 540 original and 578,433 simulated values for the middle macro-unit;
- ★ 317 original and 744,896 simulated values for the bottom macro-unit.

They are shown in the next figure just for four lithotypes, representative of the others.

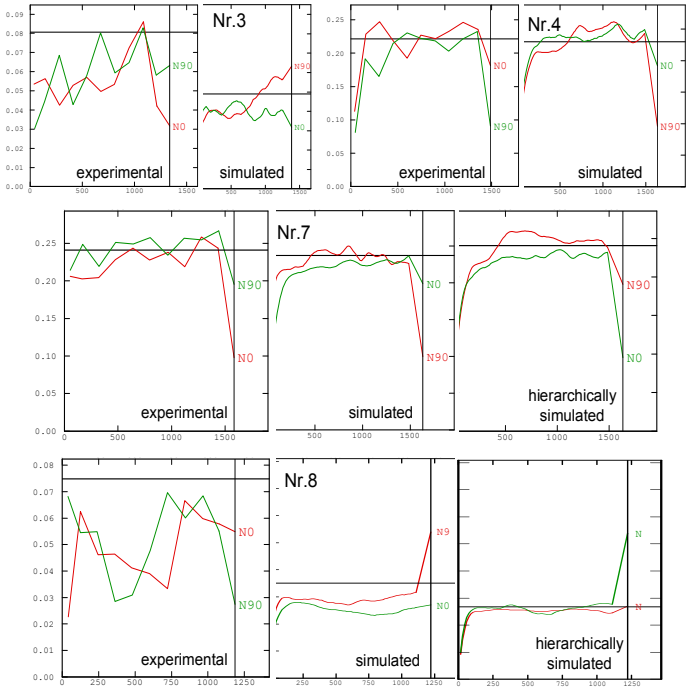

Fig. 12: Experimental and post-simulation variograms of lithotypes nr.3, 4, 7 and 8.

Almost all lithotypes show variograms like lithotypes nr.4 in Fig. 12: the simulated one is in good agreement with the experimental, in terms of both values and trend. An exception is constituted by lithotype nr.3, whose post-simulation variogram presents a sill smaller than in the experimental one, although it maintains a trend well agreeable with the experimental. The difference in the sill depends on the proportions: as it is possible to see in figure 11, the proportion of the lithotype nr.3 after the simulation is smaller than the input one. The same observation can be done for lithotypes nr.10 and 12, whose variograms are not showed.

For what concerns the middle macro-unity, two simulations have been carried out; thus for each component lithotype, indicator variables have been built from the nested simulation too. It results in three variograms to be compared. The post-simulations (nested and complete) variograms are very similar to each other and in well agreement with the experimental ones, as lithotype nr.7 shows in figure 12. While, lithotype nr.8 shows discordance: the experimental variograms is erratic, due to the small number of samples, and the variograms post-simulations have more continuous trends.

Moreover, the difference in the sills depends again on the proportions, as showed previously for lithotype nr.3.

Finally, it can be said the obtained variograms are able to well represent the spatial variability of the input data.

IV. Conclusion

The limitation of sequentially ranked categories in bigaussian simulation is overcome by means of hierarchization of the degree of anisotropy of some intrinsic characteristics of the same sedimentary formation. The possibility to distinguish within the same lithotype different levels of dishomogeneity has allowed to build up a lithostratigraphical model that in the specific case has been aimed at hydrogeological studies. Through this procedure, it has been possible to respect the original proportions and the relationships in lithotypes distribution, and, at the same time, to better focus on their sedimentological characteristics and aspects of anisotropies. This methodology can be useful in case of particularly complex lithostratigrapical reconstructions or in cases of stratigraphical gaps, heteropies of facies etc.

A check of a single simulation, based on the comparison of the experimental and post-simulation histograms and the variograms, has given good results: the simulation can be considered acceptable. In this sense, no significant differences between the two procedures of simulation (nested and complete) for the middle unity have been detected. In fact, the results of the checking procedure are almost the same. Anyway, for the considerations made previously, the nested simulations have to be considered the most correct ones. Nevertheless, the mentioned procedure cannot but be applied after accurate geologic check.

References:

[1] Dowd P.A., Pardo-Iguzquiza E., Xu C., Plurigau: a computer program for simulating spatial facies using the truncated plurigaussian method, Computers & Geosciences 29, 2003.

[2] Cherubini Claudia, Concetta I. Giasi, Fausta Musci, Nicola Pastore. Application of truncated plurigaussian method for the reactive transport modeling of a contaminated aquifer. In: Recent Advances in Water Resources, Hydraulics & Hidrology – Mathematics and Computers in Science and Engineering. Published by WSEAS Press, 2009. ISBN: 978-960-474-057-4 ISSN: 1790-2769. (ISI Book).

[3] Castrignanò A., Cherubini Claudia, Giasi C. I., Musci F., Pastore N, Multivariate Geostatistical and Natural Attenuation Model Approach for remediation of chlorinated compounds, WSEAS Transactions On Environment And Development ISSN: 1790-5079 Issue 5, Volume 3, May 2007 [ISI Transaction]

[4] Castrignanò A., Cherubini Claudia, Dima L., Giasi C. I., Musci F., The application of multivariate geostatistical techniques for the study of natural attenuation processes of chlorinated compounds, Proceedings of The 5th IASME / WSEAS International Conference (HTE'07) Vouliagmeni, Athens, Greece, August 25-27, 2007 Press ISSN: 1109-2769. ISBN: 978-960-6766-00-8 [ISI Proceedings]

[5] H. Beucher, D. Renard "Reservoir characterization". Rapport N-03/05/G, CG, Ecole des Mines de Paris.

[6] Isatis Technical reference "Plurigaussian Simulations" 2005 – Geovariances.

[7] Emery, X., Ortiz, J. M., and Cáceres, A. M., Geostatistical modeling of rock type domains with spatially varying proportions: Application to a porphyry copper deposit, Journal of the South African Institute of Mining and Metallurgy, volumen 108, n. 5, 2008 p. 285-292

[8] Betzhold, J. and Roth, C., Characterizing the mineralogical variability of a Chilean copper deposit using plurigaussian simulations, Journal of the South African Institute of Mining and Metallurgy vol. 100, n. 2, 2000, pp. 111–120.

[9] Geman, S. and D. Geman, Stochastic relaxation, Gibbs distributions,and the Bayesian restoration of images, IEEE Trans. Pattern Analysis and Machine Intelligence 6 1984 pp 721-741.

[10] Journel A.G., Ying Z., The Theoretical Links Between Sequential Gaussian Simulation, Gaussian Truncated Simulation, and Probability Field Simulation, Mathematical Geology, Volume 33, n 1, 2001, pp. 31-40(10).

[11] Chiles Jean-Paul, Delfiner Pierre Geostatistics: modeling spatial uncertainty, New York, Wiley 1999. 695 p. ISBN 0-471-08315-1.

Claudia Cherubini Graduated cum laude in 2003, PhD since 2007, currently Post Doc Scholarship at Polytechnic of Bari. Visiting Researcher in 2006 at Lawrence Berkeley National Laboratory (LBNL) and in 2005 at Geowissenschaftliches Zentrum der Universität Göttingen. Specific roles in important International Research Projects among which: Yucca Mountain Project of LBNL; European Research Project "KORA" of Universität Göttingen. European Project PRIMAC "Protection of coastal aquifers from seawater intrusion". Member of different International Scientific Committees of International Congresses, inserted in some International Program Committees, invited to be Rewiever and Speaker in the International Congresses. In 2008 didactic activity within the course "PhD International course on Advanced numerical modeling of flow and transport in soils and aquifers (ANMFT)", at University of Siena. Winner of international Prize "Best Student Paper" for the scientific paper "A hydrodynamic model of a contaminated fractured aquifer" presented at the Int. Conf. 5th IASME / WSEAS 2007. Only Italian Winner of an international selection of 35 experts in 2003. Winner of a Post doctorate Research Scholarship at University of Sannio; holder of a Post doctorate Research Scholarship at CNR. Attendance of several international training Courses. More than 40 papers published on Scientific Journals, International Books and Conference Proceedings and n. 2 final reports of European Research Projects. Some papers subject of international Selection. Certified knowledge of 6 foreign languages: English, German, Spanish, French, Portuguese and Japanese.

Fausta Musci PhD student of the "Scuola Interpolitecnica di Dottorato" (SIPD) – Area ETSC (Environmental and Territorial Safety and Control) in "Engineering and Chemistry for the safeguard of the ecosystems" Polytechnic of Bari department of Water Engineering and Chemistry. Graduated cum laude in March 2007 at First Faculty of Environmental Engineering (Polytechinc of Bari). Currently, in research period at Centre de Geosciences – Ecoles de Mines de Paris. Attendance of international course: Advanced Numerical Modeling Of Flow And Transport In Soils And Aquifers, Università degli studi di Siena, Attendance of International course "Les Méthodes de la Géostatistique: Géostatistique non-stationnaire et multivariable, Géostatistique non-linéaire et simulations", c/o Centre de Geosciences – Ecole des Mines de Paris. Attendance of the course "Simulations", part of the "**C**ycle de **F**ormation **S**pécialisée en **G**éostatistique" c/o Ecole des Mines de Paris. Research activity developed at the department of Civil and Environmental Engineering of the Polytechnic of Bari on: Geostatistical techniques applied to the hydrogeology, Geolithological and hydrogeological characterization of reservoir based on (non)linear and (non)parametric geostatistical techniques. Collaboration contract with Polytechnic of Bari Department of Civil and Environmental Engineering, about groundwater modeling on the area of Salento peninsula (Italy).

Nicola Pastore PhD student in "Engineering and Chemistry for the safeguard of the ecosystems" Polytechnic of Bari department of Water Engineering and Chemistry. Graduated in 2007 at First Faculty of Civil Engineering (Polytechinc of Bari). Attendance of international course: Advanced Numerical Modeling Of Flow And Transport In Soils And Aquifers, Università degli studi di Siena. Collaboration contract with SISTEMI INDUSTRIALI S.r.l. C.da S. Cusumano 96011 Augusta (SR) (Italy), the activities focuses on development a new groundwater cleanup technique by numerical simulation. Collaboration contract with Polytechnic of Bari Department of Civil and Environmental Engineering, about groundwater modeling on the area of Salento peninsula (Italy). Lecturer at workshop on: "Modelli di flusso nelle rocce fratturate e carsiche" October 2008, Brindisi; "Inquinamento Ambientale e Bonifiche" Tecnologie e servizi innovativi per la

gestione e prevenzione dei rischi naturali ed antropici ImpresAmbiente, Potenza. December 2008.
Research activity developed at the department of Civil and Environmental Engineering of the Polytechnic of Bari on: Modeling multiphase flow and reactive multi component transport in fractured karstic reservoir; Development of algorithms for inverse modeling problem based on fuzzy logic and global optimization techniques; Geolithological and hydrogeological characterization of reservoir based on (non)linear and (non)parametric geostatistical techniques; modeling seawater intrusion and development of remediation strategies.